Available online at www.sciencedirect.com
ScienceDirect
Acta Materialia 56 (2008) 16–22
Acta MATERIALIA
www.elsevier.com/locate/actamat

Carbon partitioning to austenite from martensite or bainite during the quench and partition (Q&P) process: A critical assessment

A.J. Clarke [a,b,*], J.G. Speer [a], M.K. Miller [c], R.E. Hackenberg [b], D.V. Edmonds [d], D.K. Matlock [a], F.C. Rizzo [e], K.D. Clarke [a], E. De Moor [f]

[a] Advanced Steel Processing and Products Research Center, Colorado School of Mines, Golden, CO 80401, USA
[b] Materials Science and Technology Division, Mail Stop G770, Los Alamos National Laboratory, Los Alamos, NM 87545, USA
[c] Materials Science and Technology Division, Microscopy, Mail Stop 6136, Oak Ridge National Laboratory, Oak Ridge, TN 37831, USA
[d] School of Process, Environmental and Materials Engineering, University of Leeds, Leeds LS2 9JT, UK
[e] Department of Materials Science and Metallurgy, Pontifícia Universidade Católica-Rio de Janeiro, RJ 22543-900, Brazil
[f] Department of Metallurgy and Materials Science, Laboratory for Iron and Steelmaking (LISm), Ghent University, Technologiepark 903, B-9052 Ghent, Belgium

Received 3 May 2007; received in revised form 7 August 2007; accepted 21 August 2007
Available online 31 October 2007

Abstract

The goal of the quench and partition (Q&P) process for steel heat treatment is to enrich austenite with carbon during a partitioning treatment after initial quenching below the martensite start temperature (M_s). Two proposed mechanisms for austenite carbon enrichment during partitioning include carbon transport from martensite and/or the formation of carbide-free bainite. Theoretical calculations show experimentally measured austenite fractions are difficult to explain based upon a mechanism involving solely bainite formation. Carbon partitioning from martensite provides a more satisfactory explanation, although the formation of bainite during partitioning cannot be completely excluded.

Keywords: Austenite; Martensite; Bainite; Atom probe tomography (APT); X-ray diffraction (XRD)

1. Introduction

The quench and partition (Q&P) process has been suggested as an alternative heat treatment to produce steels with retained austenite (γ) [1], with the added potential to tailor strength through control of martensite fraction, which forms from an initial quench below the martensite start temperature (M_s). The desired martensite fraction is obtained by quenching high temperature austenite from the austenite or the austenite plus ferrite ($\alpha + \gamma$) phase field to the desired quench temperature (QT). The martensite carbon content at QT is equal to the bulk carbon content in samples quenched from austenite, and is greater than the bulk carbon content in samples intercritically annealed prior to quenching. A subsequent partitioning treatment, which follows the initial quench to QT, is then performed to promote austenite carbon enrichment. The final amount of austenite may be modified by final cooling to room temperature, depending upon the austenite stability obtained during the partitioning treatment. Si and/or Al, which are typical additions to transformation-induced plasticity (TRIP) steel compositions, are employed to suppress carbide formation during partitioning. Q&P heat treatments have been performed on C–Mn–Si and C–Mn–Si–Al TRIP sheet steel compositions, and substantial fractions of carbon enriched retained austenite have been produced [2–5].

* Corresponding author. Address: Materials Science and Technology Division, Mail Stop G770, Los Alamos National Laboratory, Los Alamos, NM 87545, USA. Tel.: +1 505 606 2215; fax: +1 505 665 9427.
E-mail address: aclarke@lanl.gov (A.J. Clarke).

1359-6454/$30.00
doi:10.1016/j.actamat.2007.08.051

Two mechanisms by which carbon partitions to austenite during the isothermal hold at the partitioning temperature (PT) of the austenite/martensite mixture present at the QT of Q&P have been proposed, namely: (i) partitioning of carbon to untransformed austenite from carbon supersaturated martensite; and (ii) carbon enrichment of austenite associated with the formation of carbide-free bainite, especially in any large austenite pools. In this paper the two mechanisms are critically assessed through theoretical predictions, assuming either carbon partitioning from martensite or carbide-free bainite formation during the partitioning step, which are compared with direct experimental measurements of the austenite fractions produced.

2. Experimental

Q&P heat treatment of 0.19C–1.59Mn–1.63Si–0.036Al (wt.%), or 0.86C–1.58Mn–3.16Si–0.073Al (at.%), steel was performed. Intercritical annealing at 820 °C for 180 s in molten salt was first performed to produce ~25 vol.% intercritical ferrite ($\alpha_{IC} = 25\%$), resulting in approximately 0.25 wt.% carbon in the intercritical austenite. Samples were then quenched into a tin–bismuth bath at temperatures ranging from 200 to 260 °C and held for 10 s, partitioned at 400 °C in molten salt for times of 10, 30, 100 or 1000 s, and then water quenched to room temperature. The times reported are the durations that samples were submerged in each bath. Experimental austenite fractions were determined by X-ray diffraction (XRD) from chemically thinned samples [4].

Austenite and ferrite carbon concentrations, C_γ and C_α, respectively, were calculated from XRD peak positions and/or were measured by atom probe tomography (APT). APT was performed to obtain information about the amount and location of carbon within Q&P microstructures. Specimen blanks were cut from Q&P heat treated sub-sized tensile sample grip ends. The blanks were electropolished into sharp needles using a two-stage double layer technique, in combination with micropolishing that utilizes a wire loop with a drop of suspended electrolyte [6]. The respective electrolytes used were 25% perchloric acid (70%) in glacial acetic acid and 2% perchloric acid in 2-butoxyethanol [6]. For the APT analyses, the specimen temperature was 60 K, and a pulse fraction of 20% and pulse repetition rate of 200 kHz were used.

Theoretical retained austenite amounts anticipated after partitioning were calculated assuming full partitioning of carbon from martensite to austenite during Q&P processing, or by assuming carbide-free bainite formation during partitioning. Details regarding the partitioning-from-martensite calculations, where carbon partitioning from martensite to austenite is considered, are provided in the literature [3,4,7,8]. The partitioning-from-bainite calculations that assume carbide-free bainite formation at the partitioning temperature from austenite present at the QT incorporated experimental C_γ and C_α values determined from XRD and/or APT. The APT experimental ferrite carbon concentration values used in the calculations presented in this paper represent both the martensite carbon concentration when considering the process of carbon partitioning from martensite, and the bainite carbon concentration when considering carbide-free bainite formation for enriching austenite. The details of the calculations that assume austenite enrichment by carbide-free bainite formation during the partitioning step are presented below.

The amount of martensite and austenite at each quench temperature (prior to partitioning of carbon during the partitioning step) was predicted using the Koistinen–Marburger relationship [9,10]:

$$f_m^{QT} = 1\text{–}e^{-1.1\times10^{-2}(M_s - QT)} \tag{1}$$

where f_m^{QT} is the fraction of austenite that transforms to martensite upon quenching to a temperature QT (°C) below the M_s temperature (°C). f_γ^{QT} is the fraction of austenite remaining at QT, and is given by $1 - f_m^{QT}$. Corrections for the amount of intercritical ferrite were applied.

The fractions of austenite and bainitic ferrite that would be associated with bainite formation during partitioning were determined by applying the lever-rule using experimentally determined ferrite carbon concentration and the initial and final austenite carbon concentrations. The fractions of bainitic ferrite and austenite are given by the mass balance expressions:

$$f_\alpha^b = \left(\frac{C_\gamma - C_\gamma^{IC}}{C_\gamma - C_\alpha}\right) * f_\gamma^{QT} \quad \text{and}$$
$$f_\gamma^b = \left(\frac{C_\gamma^{IC} - C_\alpha}{C_\gamma - C_\alpha}\right) * f_\gamma^{QT} \tag{2}$$

where f_α^b and f_γ^b are the fractions of ferrite and austenite, respectively, associated with the formation of carbide-free bainite, C_γ is the experimentally determined retained austenite carbon content, C_γ^{IC} is the carbon content (~0.25 wt.%) of the initial austenite (intercritical in this instance) before quenching, C_α is the (bainitic) ferrite carbon content and f_γ^{QT} is the fraction of austenite present at the quench temperature QT, or the fraction of the microstructure still available for transformation to bainite during partitioning.

For these calculations, a range of retained austenite carbon levels obtained from XRD and/or APT results were used, from 0.73 to 1.35 wt.% (~3.3 to ~5.9 at.%). The bainitic ferrite was assumed to have an average carbon content of 0.10 or 0.04 wt.% (~0.46 or ~0.18 at.%), based on measurements from low carbon lath regions of two different three-dimensional carbon atom maps obtained from APT of Q&P heat treated samples.[1] Recently, Caballero

[1] Microstructures produced by Q&P and examined by transmission electron microscopy (TEM) contained lath regions presumed to be martensite and interlath austenite films [3,4]. The low carbon lath regions observed in the carbon atom maps are presumed to be martensite laths, but are hypothetically treated as bainitic ferrite for these calculations.

et al. reported carbon concentrations in austenite and bainitic ferrite for a 0.98 C–1.46Si–1.89Mn–0.26Mo–1.26Cr–0.09 V (wt.%), or 4.34 C–2.76Si–1.82Mn–0.14Mo–1.28Cr–0.09 V (at.%), steel obtained with XRD and/or APT after isothermal holding at 200 or 300 °C [11,12]. Processing differed from the current work, where two-stage heat treatment was employed. The average austenite carbon content of 6.60 ± 0.44 at.% was determined by XRD for the 200 °C condition, whereas the local carbon content 5.39 ± 0.18 at.% was determined by APT [11]. Similarly, austenite carbon levels of 5.67 ± 0.44 and 6.85 ± 0.22 at.% were determined by XRD and APT, respectively, for the 300 °C condition [11]. The bainitic ferrite carbon contents reported were 2.92 ± 0.30 at.% for 200 °C and 1.37 ± 0.30 at.% for 300 °C by XRD, whereas the carbon levels reported for APT were 0.62 ± 0.10 at.% for 200 °C and 0.52 ± 0.04 at.% for 300 °C [11]. XRD provides the average carbon content, which would include the contribution of local regions enriched with carbon, such as carbon trapped at dislocations. Carbon trapping by dislocations in bainitic ferrite has been reported, especially in regions near ferrite/austenite interfaces [11]. Carbon concentration results obtained using APT would not include the contribution of these local carbon enriched regions, unless specifically observed in three-dimensional carbon atom maps and included in carbon concentration analyses. Excluding local carbon enriched regions likely resulted in an underestimation of (bainitic) ferrite carbon content using the APT technique. For the calculations considering bainite formation in the present work, the bainitic ferrite carbon contents of 0.10 and 0.04 wt.% obtained by APT might be lower than expected from XRD. Thus, it should be noted that underestimation of bainitic ferrite carbon concentration with the APT technique would result in the overestimation of calculated austenite fractions, in the case where austenite carbon enrichment is a result of a bainite transformation mechanism.

Two different experimental carbon concentration levels (0.10 and 0.04 wt.%) were selected to represent bainitic ferrite carbon contents, in order to show the effect of carbon level on calculated austenite fractions. The carbon level 0.10 wt.% represents a condition of ferrite with some modest carbon supersaturation commonly reported for bainite [11–15], which is typically associated with displacive transformation models, where ferrite initially forms with carbon supersaturation, followed by escape of carbon from the newly formed ferrite to austenite [11–17].

Low carbon levels (<0.02 wt.%) are expected for intercritical ferrite, which further supports that the low carbon lath regions observed in the carbon atom maps are either bainitic ferrite, provided that the bainitic ferrite is supersaturated with some carbon, or carbon-depleted martensite.

The details of these calculations that determine the fraction of bainitic ferrite and retained austenite associated with bainite formation during the partitioning treatment are further highlighted in the following example, where $C_\gamma^{IC} = 0.253$ (wt.%) since $\alpha_{IC}=0.25$ vol. fraction, and $C_\gamma = 1.09$ (wt.%) and $f_\gamma^{QT} = 0.113$ after quenching to 200 °C and holding for 10 s and partitioning at 400 °C for 10 s. For this example, M_s is ~372 °C, determined from the empirical expression [18]:

$$M_s(^\circ\mathrm{C}) = 539 - 423\mathrm{C} - 30.4\mathrm{Mn} - 7.5\mathrm{Si} + 30\mathrm{Al} \quad (3)$$

where C, Mn, Si and Al are the contents of these elements in wt.%. Using the appropriate values, this yields $f_\alpha^b = 0.096$ and $f_\gamma^b = 0.017$ for $C_\alpha = 0.10$ (wt.%) and $f_\alpha^b = 0.09$ and $f_\gamma^b = 0.023$ for $C_\alpha = 0.04$ (wt.%).

There has been significant debate regarding the specific mechanism of bainite formation (i.e. displacive, diffusional or diffusional–displacive) [13,16,17,19–25], and it must be recognized that the goal of these calculations is not to clarify the mechanism of bainite formation but, rather, to determine if the experimentally obtained levels of enriched austenite are possible if bainite formation is the sole, or primary, process for austenite enrichment.

3. Results and discussion

Experimental austenite fractions (Fig. 1a) and carbon contents (Fig. 1b) as a function of partitioning time for the indicated QT and PT values are shown in Fig. 1. The maximum austenite fractions of ~0.11 and ~0.10 obtained for the 200 and 220 °C quench temperature series, respectively, were obtained after partitioning for 10 s. Partitioning for longer times decreased the amount of austenite that was retained for these two quench temperatures (200 and 220 °C). The maximum austenite fraction was retained at 30 s for the 240 °C quench temperature, while the maximum austenite fraction was achieved at 100 s for the 260 °C quench temperature. At the longest partitioning time examined (1000 s), the lowest austenite fraction was obtained for each quench temperature series, which could be due to the competing processes of carbide formation or perhaps the simple consumption of significant amounts of austenite by bainitic ferrite. However, bainite formation, a possible mechanism for austenite enrichment operating during the partitioning treatment and explored by the theoretical austenite fraction calculations in this paper, would also be expected to promote austenite carbon enrichment, which is not clearly reflected in the results shown in Fig. 1b after 1000 s.

The maximum level of carbon enrichment in austenite (~1.3 wt.%) was obtained after partitioning for 100 s for each quench temperature examined (Fig. 1b). After partitioning for 1000 s at 400 °C for the QT's examined, less austenite enrichment was observed, potentially due to carbide formation at this long partitioning time. In related studies [3,4], carbides were observed using TEM after partitioning for 30 s or greater at 400 °C in some samples.

A sample three-dimensional carbon atom map obtained from APT, showing the amount and location of carbon in a Q&P microstructure after Q&P heat treatment, illustrates

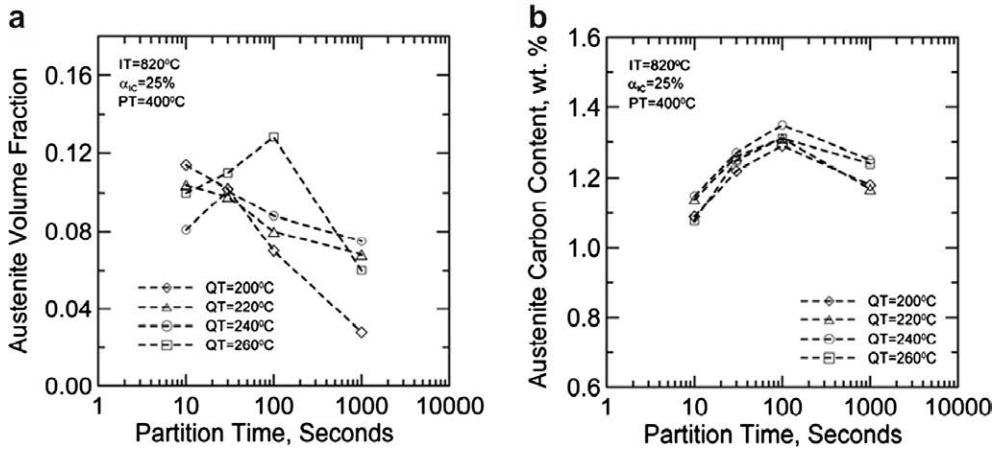

Fig. 1. Open symbols show austenite fraction (a) and corresponding austenite carbon content (b) obtained by XRD for Q&P samples as a function of partition time after intercritical annealing at 820 °C for 180 s, quenching to 200, 220, 240 or 260 °C and holding for 10 s, partitioning for 10, 30, 100 or 1000 s at 400 °C and then water quenching to room temperature. IT = 820 °C designates the intercritical annealing temperature, $\alpha_{IC} = 25\%$ designates the approximate intercritical ferrite amount, PT = 400 °C designates the partitioning temperature and QT = 200, 220, 240 or 260 °C designates the quench temperature.

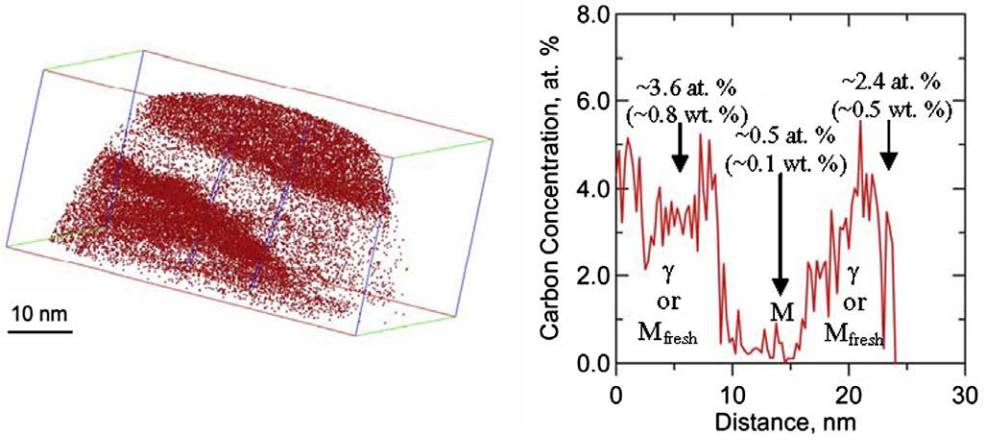

Fig. 2. A carbon atom map from a sample intercritically annealed at 820 °C for 180 s, quenched to 220 °C and held for 10 s, and then partitioned at 400 °C for 10 s before water quenching to room temperature. The large box (left) is $56 \times 55 \times 27$ nm^3 and the smaller box within it shows a region selected for carbon concentration analysis (right). The low carbon region (M) is presumed to be low carbon martensite. The high carbon regions are presumed to be retained austenite (γ), or possibly fresh martensite (M_{fresh}) that formed on final cooling to room temperature after the partitioning treatment or during the cryogenic cooling required for the APT experiment. The average austenite carbon content determined from XRD was ~1.1 wt.% for this condition, and the austenite amount was determined to be ~10.4%.

carbon enriched regions and a low carbon region in Fig. 2.[2] The average carbon concentration through the low carbon region for the example shown was determined to be ~0.10 wt.% after averaging with a value obtained from another profile through the same region; the average austenite carbon concentration through the carbon enriched regions was determined to be ~0.73 wt.%; the lowest austenite carbon level used in the present calculations. The average carbon content obtained from XRD for this condition was ~1.1 wt.%. Average carbon concentration values for the low and high carbon regions for one carbon concentration profile obtained from APT are provided in Fig. 2. The low carbon region, designated M in Fig. 2, is presumed to be low carbon martensite. The high carbon regions are presumed to be austenite in this example, although based on their carbon concentration may have partially transformed to high carbon, fresh martensite on final cooling to room temperature after the partitioning treatment, or especially during the cryogenic cooling to 60 K required

[2] In addition to showing the amount and location of carbon in Q&P microstructures, APT was also performed to specifically examine carbon gradients extending into the austenite from austenite/martensite interfaces as a function of partitioning time for direct comparisons with calculated carbon partitioning kinetics. Results from these simulations [3,4] are not presented here, however.

for the APT experiment. Thus, in Fig. 2 the carbon enriched regions are designated as γ or M_{fresh}, corresponding to austenite or high carbon, fresh martensite. In either case, the APT results in Fig. 2 provide direct supporting evidence for austenite enrichment by Q&P processing.

Theoretical austenite predictions for the two processes for austenite carbon enrichment (partitioning from martensite or carbide-free bainite formation) are plotted in Fig. 3. Austenite fractions calculated assuming bainite formation during the partitioning step are shown as inverted triangles. As previously mentioned, ferrite carbon concentrations of 0.10 or 0.04 wt.% were used in the calculations with austenite carbon concentrations determined by XRD and/or APT. The two solid inverted triangles in Fig. 3 were calculated with ferrite and austenite carbon concentrations obtained from APT data. The other calculated austenite fractions that assume bainite formation (open inverted triangles) were calculated with austenite carbon concentrations obtained from XRD and ferrite carbon concentrations obtained from APT data. Average austenite carbon contents obtained from XRD were often similar to local levels obtained using APT for conditions where both techniques were employed.

Recall that bainitic ferrite carbon content could be underestimated by the APT technique if compared with average carbon content values obtained from XRD. For the calculations considering bainite formation described in this paper, a similar trend would result in the overestimation of the calculated austenite values shown in Fig. 3. All of the calculated austenite fractions that assume bainite formation in Fig. 3 are low, because much of the available austenite transforms to martensite during the initial quench. Then, any remaining austenite that would transform to a mixture of carbide-free bainite plus retained austenite necessarily leads to a significant fraction of bainitic ferrite, with only a small amount of final austenite remaining to be stabilized. The kinetics of bainite formation are not specifically considered in this approach, but are implicitly included in the calculated fractions of austenite and bainitic ferrite (through the measured carbon enrichment levels), since times ranging from 10 to 1000 s were investigated by XRD and/or APT for the partitioning temperature.

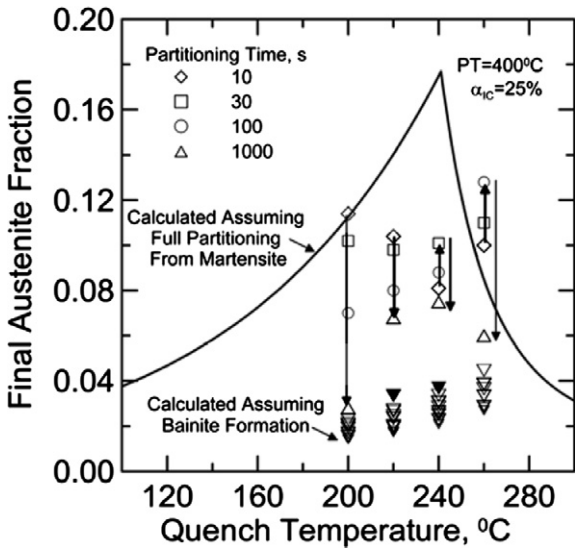

Fig. 3. Comparison of experimental austenite fractions (open symbols, not including inverted triangles) with calculated austenite fractions assuming two different possible mechanisms for austenite stabilization. A calculated [3,4,7,8] theoretical final austenite fraction curve (solid line) is shown based upon idealized full partitioning of carbon to austenite from martensite during Q&P processing. Calculated austenite fractions (open and solid inverted triangles) that assume carbide-free bainite formation are also shown. The two solid inverted triangles were calculated with carbon concentrations for both austenite and ferrite obtained from APT data. The other calculated austenite fractions (open inverted triangles) were calculated with austenite carbon concentrations obtained from XRD and ferrite carbon concentrations obtained from APT data. PT = 400 °C designates the partitioning temperature and $\alpha_{IC} = 25\%$ designates the intercritical ferrite amount.

A theoretical final austenite fraction curve (solid line), calculated based upon full partitioning of carbon from martensite to austenite during Q&P processing is also shown in Fig. 3 [4]. The theoretical final austenite fraction curve was calculated [3,4,7,8] by application of the Koistinen–Marburger relationship [9,10] to both the initial quenching and the final quenching step to room temperature (~25 °C) after idealized full partitioning. It is assumed in this simplified model that all of the carbon partitions to the austenite and partitioning is complete (i.e. all carbon migrates to the austenite and the kinetics of partitioning are ignored). Implicit in this analysis is that there are no competing reactions, such as carbide formation or carbon segregation to dislocations in martensite. Based on full partitioning, an optimum QT of approximately 240 °C is predicted to maximize the austenite content.

Experimental austenite fractions determined from XRD are also shown in Fig. 3 (open symbols, not including inverted triangles), illustrating the experimentally obtained partitioning kinetics for several different quench temperatures examined, ranging from 200 to 260 °C. The arrows highlight increased partitioning time.[3] The theoretical final austenite fraction curve, calculated assuming idealized full partitioning of carbon to austenite from martensite, actually predicts lower fractions of austenite than the experimental values at high quench temperatures; the higher fractions observed are presumably due to kinetic effects [3,4]. Experimental values below the calculated curve likely reflect incomplete partitioning or competing processes, such as carbide formation or carbon segregation to dislocations in martensite.

The comparisons in Fig. 3 show that all of the experimental austenite fractions measured with XRD are significantly higher (by factors of about 2–4) than the values predicted based on bainite formation. This comparison suggests that bainite formation alone cannot be responsible

[3] The time dependence for austenite stabilization is considered to be associated with carbon gradients that develop within austenite films as partitioning time increases, which is further addressed and discussed in Refs. [3,4].

for the experimental levels of enriched austenite and, thus, is not the primary process for austenite stabilization during Q&P processing. For example, 10 s of partitioning for the quench temperature 200 °C resulted in an experimental austenite fraction of ~0.11, whereas bainite formation with the level of austenite enrichment obtained (~1.1 wt.% C from XRD) would result in a retained austenite fraction of only ~0.02, clearly much less than that shown in Fig. 3 for this condition. Reduced carbon concentrations in the bainitic ferrite, such as ~0.02 wt.%, would result in slightly higher austenite fractions than the calculated values (inverted triangles) shown in Fig. 3, but still would not account for the measured levels of enriched retained austenite.

The theoretical, maximum final austenite fraction possible associated with the formation of bainite from the austenite present at each QT was calculated considering the ferrite and austenite concentrations that would give the largest lever-rule austenite amount. Eq. (3) was used to determine the austenite carbon level required for austenite to have an M_s of, and therefore be stable at, room temperature (25 °C). An M_s below room temperature would also result in stable austenite at room temperature. Without partitioning of the substitutional alloying additions, austenite would need to have a carbon level of nearly 1.1 wt.% (~1.075 wt.%) for this condition to be satisfied. Using this carbon level for the austenite and zero carbon for the bainitic ferrite (i.e. all carbon goes to retained austenite, which represents the maximum possible enrichment via bainite formation), the maximum austenite fractions possible are ~0.026, ~0.033, ~0.041 and ~0.051 for quench temperatures of 200, 220, 240 and 260 °C, respectively. This approach ignores any carbon gradients that may be present in the austenite. The values are slightly higher than the final austenite fractions calculated assuming bainite formation using the experimental austenite and ferrite enrichment levels (inverted triangles in Fig. 3), but remain substantially lower than the experimental austenite fractions. The requirement that the austenite carbon level reach ~1.1 wt.% further suggests that the austenite in the carbon atom map of Fig. 2 likely transformed partly to fresh martensite, but nevertheless still provides evidence of significant austenite carbon enrichment during Q&P. The average austenite carbon levels reported from XRD provided in Fig. 1b certainly approach ~1.1 wt.% carbon or greater, however, indicating stability at room temperature.

The calculated maximum final austenite fractions described above, where the austenite needs to achieve sufficient stability to avoid transformation to fresh martensite on final quenching or cooling to room temperature, are controlled by the phase compositions "independently" of the mechanism of bainite formation, but some comments may be warranted in this regard.

For bainite growth by a displacive mechanism [13,16], bainite formation stops when the austenite reaches a carbon level near T_0, the carbon level at a particular temperature where the free energy of ferrite and austenite are equivalent. If strain energy and Zener ordering are considered, the carbon level of interest for a given temperature is designated T'_0. Both T_0 and T'_0 values have been calculated [26] for the steel composition examined in this work. At 400 °C, the calculated T_0 and T'_0 values are 3.86 at.% (~0.87 wt.%) and 2.7 at.% (~0.61 wt.%) carbon, respectively. These carbon levels are lower than required for the austenite to be stable at room temperature, as described previously. Thus, if T_0 or T'_0 values are used to represent the carbon level of the austenite, very little austenite would be anticipated to remain after quenching to room temperature.

Hillert has reported that bainite in a 0.4C–3.00Mn–2.12Si (wt.%) steel appears to grow under no partition, local equilibrium (NPLE) conditions at high temperatures [21], where bainitic ferrite grows without carbon supersaturation and negligible partitioning of substitutional elements, and approaches growth under paraequilibrium conditions at low temperatures [21]. If the calculated [26] paraequilibrium value of ~3 wt.% (12.5 at.%) for this steel was used to represent the austenite carbon concentration and zero carbon was assumed in the bainitic ferrite, austenite fractions lower than those shown by the inverted triangles in Fig. 3 would be obtained. NPLE carbon concentration values were not calculated in this work, but if the value of ~0.56 wt.% (~2.5 at.%) [21] at ~400 °C for the 0.4C–3.00Mn–2.12Si (wt.%) steel considered by Hillert was used as an approximation, the austenite stability would be insufficient to avoid partial transformation to fresh martensite at room temperature. Thus, regardless of the presumed mechanism of bainite formation, the calculated austenite fractions that assume bainite formation from the austenite available at each QT cannot reach the levels of austenite measured experimentally.

Based upon the austenite fractions calculated in comparison with experimental values, the results support the operation of carbon partitioning to austenite from martensite, since carbon partitioning from martensite provides a more satisfactory explanation than the formation of carbide-free bainite for the mechanism of austenite enrichment during Q&P processing. The formation of some bainite during partitioning cannot be completely excluded, however, since the results only support the conclusion that bainite formation alone cannot explain the experimental austenite fractions and levels of enrichment.

4. Conclusions

The austenite fractions calculated assuming only bainite formation during quenching and partitioning are insufficient to explain the levels of enriched austenite observed experimentally. In the case of the theoretical bainite formation process, too much austenite is consumed in producing martensite (during the initial quench) and then bainitic ferrite to stabilize the levels of austenite measured experimentally. Consequently, the partitioning of carbon to austenite from the initial martensite is more consistent with the experimental austenite fraction results. In this case, the

absence of bainitic ferrite leaves more untransformed austenite that can be stabilized by carbon during partitioning. In this instance, deviation from the predicted results is then indicative of incomplete partitioning, for example, loss of carbon atoms to competing processes, mainly thought to be carbide precipitation or the segregation of carbon atoms to dislocations, although some carbide-free bainite formation could also be a competing process to reduce the final austenite fraction below the theoretically predicted level.

Acknowledgements

The authors gratefully acknowledge the support of the Advanced Steel Processing and Products Research Center, a National Science Foundation Industry/University Cooperative Research Center at the Colorado School of Mines (CSM) and the Inter-American Materials Collaboration Program. A.J.C. and R.E.H. acknowledge support from the US Department of Energy (contract DE-AC52-06NA25396) during the preparation of this manuscript. Funding is acknowledged from NSF award #0303510 (USA), CNPq (Brazil) and EPSRC (United Kingdom). Research at the Oak Ridge National Laboratory (ORNL) SHaRE User Facility was sponsored by the Division of Scientific User Facilities, Office of Basic Energy Sciences, US Department of Energy, under contract DE-AC05-00OR22725 with UT-Battelle, LLC. K.F. Russell at ORNL and K. He at the University of Leeds are gratefully acknowledged for their assistance with the APT and TEM, respectively. E.J. Pavlina, M.C. Mataya and C.J. Van Tyne at CSM are thanked for helpful discussions, and POSCO is gratefully acknowledged for providing the experimental material.

References

[1] Speer JG, Matlock DK, De Cooman BC, Schroth JG. Acta Mater 2003;51:2611.
[2] Streicher AM, Speer JG, Matlock DK, De Cooman BC. In: Speer JG, editor. Proceedings of the International Conference on Advanced High-strength Sheet Steels for Automotive Applications. Warrendale, PA: AIST, 2004. p. 51.
[3] Clarke A, Speer JG, Matlock DK, Rizzo FC, Edmonds DV, He K. In: Howe Laughlin DE, Lee JK, Dahmen U, Soffa WA, editors. Solid–solid Phase Transformations in Inorganic Materials 2005, vol. 2. Warrendale, PA: TMS; 2005. p. 99.
[4] Clarke A. Carbon partitioning into austenite from martensite in a silicon-containing high-strength sheet steel. Ph.D. Thesis. Golden, CO: Colorado School of Mines, 2006.
[5] De Moor E, Lacroix S, Samek L, Penning J, Speer JG. In: Chung J-Y, Naoki O, Weng Y, editors. The 3rd International Conference on Advanced Strength Steels. Gyeongju: Korean Institute for Metals and Materials, 2006. p. 873.
[6] Miller MK. Atom Probe Tomography Analysis at the Atomic Level. New York: Kluwer Academic/Plenum Publishers; 2000.
[7] Speer JG, Streicher AM, Matlock DK, Rizzo F, Krauss G. In: Damm EB, Merwin M, editors. Austenite formation and decomposition. Warrendale, PA: ISS/TMS; 2003. p. 505.
[8] Speer JG, Edmonds DV, Rizzo FC, Matlock DK. Curr Opin Solid State Mater 2004;8:219.
[9] Koistinen DP, Marburger RE. Acta Metall 1959;7:59.
[10] Krauss G. Steels: Heat Treatment and Processing Principles Metals. Park, OH: ASM International; 1990.
[11] Caballero FG, Miller MK, Babu SS, Garcia-Mateo C. Acta Mater 2007;55:381.
[12] Caballero FG, Miller MK, Babu SS, Garcia-Mateo C, Garcia de Andrés C. In: Howe Laughlin DE, Lee JK, Dahmen U, Soffa WA, editors. Solid–solid Phase Transformations in Inorganic Materials 2005, vol. 1. Warrendale, PA: TMS; 2005. p. 511.
[13] Bhadeshia HKDH. Bainite in Steels. 2nd ed. London: IOM Communications; 2001.
[14] Peet M, Babu SS, Miller MK, Bhadeshia HKDH. Scripta Mater 2004;50:1277.
[15] Pereloma EV, Timokhina IB, Miller MK, Hodgson PD. Acta Mater 2007;55:2587.
[16] Bhadeshia HKDH, Christian JW. Metall Trans A 1990;21A:767.
[17] Mujahid SA, Bhadeshia HKDH. Acta Metall Mater 1992;40:389.
[18] Mahieu J, Maki J, De Cooman BC, Claessens S. Metall Mater Trans A 2002;33A:2573.
[19] Hillert M, Höglund L, Ågren J. Acta Metall Mater 1993;41:1951.
[20] Aaronson HI, Reynolds Jr WT, Shiflet GJ, Spanos G. Metall Trans A 1990;21A:1343.
[21] Hillert M. Metall Mater Trans A 1994;25A:1957.
[22] Ågren J. Acta Metall 1989;37:181.
[23] Olson GB, Bhadeshia HKDH, Cohen M. Acta Metall 1989;37:381.
[24] Olson GB, Bhadeshia HKDH, Cohen M. Metall Trans A 1990;21A:805.
[25] Mujahid SA, Bhadeshia HKDH. Acta Metall Mater 1993;41:967.
[26] Bhadeshia HKDH. Materials Algorithms Project. Program MAP_STEEL_MUCG46. <http://www.msm.cam.ac.uk/map/steel/programs/mucg46-b.html>.